Formation and structure of stable aggregates in binary diffusion-limited cluster-cluster aggregation processes

J. M. López-López, A. Moncho-Jordá, A. Schmitt, and R. Hidalgo-Álvarez*
Biocolloid and Fluid Physics Group, Department of Applied Physics, University of Granada, Campus de Fuentenueva, E-18071 Granada, Spain
(Received 23 December 2004; revised manuscript received 9 May 2005; published 1 September 2005)

Binary diffusion-limited cluster-cluster aggregation processes are studied as a function of the relative concentration of the two species. Both, short and long time behaviors are investigated by means of three-dimensional off-lattice Brownian Dynamics simulations. At short aggregation times, the validity of the Hogg-Healy-Fuerstenau approximation is shown. At long times, a single large cluster containing all initial particles is found to be formed when the relative concentration of the minority particles lies above a critical value. Below that value, stable aggregates remain in the system. These stable aggregates are composed by a few minority particles that are highly covered by majority ones. Our off-lattice simulations reveal a value of approximately 0.15 for the critical relative concentration. A qualitative explanation scheme for the formation and growth of the stable aggregates is developed. The simulations also explain the phenomenon of monomer discrimination that was observed recently in single cluster light scattering experiments.

DOI: 10.1103/PhysRevE.72.031401 PACS number(s): 82.70.Dd, 61.43.Hv, 05.40.−a

I. INTRODUCTION

Aggregation processes have been the subject of a large number of theoretical and simulation studies due to their importance for many industrial applications and natural phenomena. Most of these works focus on initially monodisperse one-component systems. In real systems, however, such ideal cases are rarely found. Moreover, naturally occurring aggregation processes usually involve mixtures of entities with different properties.

In the present work, we study the aggregation behavior of one of the simplest examples of such a multi-component system. Our system is formed by two types of equally sized colloidal particles. We assume the particles to diffuse freely and to react on contact such that only collisions between unlike particles lead to bond formation. This aggregation scheme is known as binary diffusion-limited cluster-cluster aggregation (BDLCA) [1]. Although it supposes a very ideal case of aggregation processes arising in multi-component systems, it will allow basic aspects of such processes to be studied and analyzed. Moreover, it may even serve to model real systems such as electrostatic heteroaggregation of mixtures of positively and negatively charged particles when the electric interactions are sufficiently screened but not completely suppressed. In this case, only short-range repulsive and attractive interactions between like and unlike particles are present. Hence, the interactions control the stickiness of the particles but are not expected to alter their diffusivity.

Pioneering BDLCA simulations were performed by Meakin and Djordjević [2]. They studied 10000 monomers that occupy the cells of a cubic lattice at a volume fraction of $\phi=0.0048$. In their work, all clusters performed a random walk with a size-independent diffusivity. They found that only relatively small aggregates are formed when the initial relative concentration of the minority particles, x, lies below a critical value. In this case, all the minority particles achieve to be contained in small aggregates that are completely coated with majority particles. Evidently, these aggregates cannot react anymore with other majority particles and so, aggregation comes to an end. Stoll and Pefferkorn [3] performed more realistic simulations considering a size-dependent cluster diffusivity. The small number of particles used by these authors, however, does not allow them to extract reliable conclusions concerning dynamical quantities.

Recently, exhaustive on-lattice simulations performed by AlSunaidi *et al.* [1] confirmed the existence of such a critical relative concentration, x_c, separating two different aggregation regimes. For $x>x_c$, aggregation continues until a unique large cluster containing all the particles is formed. For $x<x_c$ more than one stable cluster remains in the system. They reported a value of x_c around 0.2. Nevertheless, on-lattice simulations limit bond formation to only a few sites on the particle surface. This quite unrealistic geometric constraints for the cluster structure implies that the size of the stable aggregates becomes restricted to 7, 12, 13, etc. if a cubic lattice is used. Meakin and Djordjević already mentioned the necessity of performing off-lattice simulations in order to avoid this unrealistic geometric constraint [2]. The highly expensive computer time, however, dissuaded them from performing off-lattice simulations.

Nowadays, the worthy improvement in computer technology made it possible to carry out off-lattice BDLCA simulations spending a reasonable time. Puertas *et al.* performed such off-lattice simulations. They also included long-range attractive and repulsive particle-particle interactions [4]. Nevertheless, these long-range interactions imply that their system is not diffusion-controlled and so does not correspond to a BDLCA process. In addition, as they focus mainly on the short time kinetics, stable aggregates were not reported. Table I summarizes the main characteristics of the works reviewed here.

*Electronic address: rhidalgo@ugr.es

TABLE I. Main characteristics of some two-component aggregation simulations, initial number of monomers N_0, volume fraction ϕ, diffusivity of an i-sized cluster D_i, and on/off-lattice performance.

Work	N_0	ϕ	D_i/D_1	Lattice
Meakin (1986) [2]	10000	0.0048	1	Cubic
Stoll (1993) [3]	1000	0.0034	i^{γ}	Cubic
AlSunaidi (2000) [1]	500000	0.010	$a/R_g(i)$	Cubic
Puertas (2001) [4]	2000	0.0010	$a/R_g(i)$	Off lattice
This work	25000	0.0001	$a/R_g(i)$	Off lattice

The aim of this work is to study binary diffusion-limited cluster-cluster aggregation processes by means of off-lattice simulations. Both, the short and long time kinetics will be investigated as a function of the initial relative concentration of the two species. We especially focus on the formation and growth of the stable aggregates that are expected at low relative concentration. Kinetic and structural aspects will be discussed and contrasted with the results reported in the literature for on-lattice simulations.

This paper is organized as follows: Section II reports the theoretical background. Section III briefly describes the simulations. In Section IV, the simulation results are reported for both, short and long aggregation times. Furthermore, a simple scheme for the off-lattice BDLCA kinetics is proposed. Finally, Sec. V summarizes the conclusions.

II. THEORETICAL BACKGROUND

Aggregation processes are frequently described by means of the cluster-size distribution (CSD), $n_i(t)$, which gives the number of aggregates composed by i particles at the time t. For dilute systems and irreversible aggregation, the CSD is given by the well-known Smoluchowski coagulation equation [5,6],

$$V\frac{dn_i}{dt} = \frac{1}{2}\sum_{j=1}^{i-1} k_{j,i-j} n_j n_{i-j} - n_i \sum_{j=1}^{\infty} k_{ij} n_j, \tag{1}$$

where V is the total volume of the system. The first term on the right-hand side (rhs) of Eq. (1) accounts for all reactions that create i-size clusters and so, is called birth term. The second term, or death term, quantifies the disappearance of i-size clusters due to reactions with other clusters. All physical information about the aggregation process is contained in the set of aggregation rate constants, k_{ij}, usually known as the kernel of the system.

In order to extend such a description to two-component systems, not only the number of clusters composed by i particles, but also their internal composition is required. Accordingly, we define the composition-detailed cluster size distribution (CDCSD), n_i^l, as the number of clusters composed by i particles, being l of them of the minority type. The CDCSD is straightforwardly related with the nondetailed CSD, since $\Sigma_{l=0}^{i} n_i^l = n_i$. Analogously, we define k_{ij}^{lm} as the aggregation rate constant controlling the aggregation of an i-size cluster containing l minority particles and a j-size cluster containing m minority particles. The corresponding aggregation equation reads

$$V\frac{dn_i^l}{dt} = \frac{1}{2}\sum_{j=1}^{i-j}\sum_{m=0}^{j} k_{j,i-j}^{m,l-m} n_j^m n_{i-j}^{l-m} - n_i^l \sum_{j=1}^{\infty}\sum_{m=0}^{j} k_{ij}^{lm} n_j^m. \tag{2}$$

It should be noted that $n_i^l(t)$ does not contain information on the internal structure. Hence, the rate constants k_{ij}^{lm} must be understood as averages over all possible spatial configurations.

Equations (1) and (2) can be solved analytically only for a few special kernels with certain initial conditions [7]. As will be mentioned in Sec. III, all the simulations performed in this work started from monomeric initial conditions, i.e., $n_i^l(t=0) = \delta_{i1} N_0[\delta_{l0}(1-x) + \delta_{l1} x]$, where N_0 is the total number of particles in the system, $0 \leqslant x \leqslant \frac{1}{2}$ is the relative concentration of the interacting species and δ_{ij} is the Kronecker delta.

Evidently, the most probable reaction during the early stages of all aggregation processes starting from monomeric initial conditions (including BDLCA processes) is dimer formation. Consequently, the dimer formation rate constants, k_{11}^{lm}, play the predominant role here. Hogg, Healy, and Fuerstenau exploited this fact for deriving an approximation for the monomer number evolution in binary heteroaggregation processes in the zero time limit [8]. It is known as the HHF approximation and is given by

$$V\frac{dn_1}{dt} = -k_s (n_1)^2, \tag{3}$$

where k_s is an effective dimer formation rate constant given by

$$k_s = (1-x)^2 k_{11}^{00} + x^2 k_{11}^{11} + 2x(1-x) k_{11}^{10}. \tag{4}$$

The effective dimer formation rate constant also provides an adequate time scale for binary aggregation processes. Thus, the aggregation time is defined as

$$t_{\mathrm{agr}} = \frac{2V}{N_0 k_s}. \tag{5}$$

In BDLCA processes, reactions between like particles are not allowed, i.e., $k_{11}^{00} = k_{11}^{11} = 0$. Therefore, Eq. (4) now reads as follows:

$$k_s = 2x(1-x) k_{11}^{10}. \tag{6}$$

Since aggregation between unlike particles is just due to Brownian diffusion, the rate constant k_{11}^{10} should just be the Smoluchowski rate constant k_{11}^{Br} [6],

$$k_{11}^{\mathrm{Br}} = \frac{8}{3}\frac{k_B T}{\eta}, \tag{7}$$

where k_B is the Boltzmann constant, T is the temperature and η is the viscosity of the medium. For water at $T = 293$ K, one obtains $k_{11}^{\mathrm{Br}} = 10.79 \times 10^{-18}$ m^3 s^{-1}.

III. SIMULATION DETAILS

Extensive three-dimensional (3D) off-lattice Brownian simulations with periodic boundary conditions were per-

formed. Initially, $N_0=25\,000$ spherical particles of radius $a=1$ were randomly scattered in a cubic box of side L, avoiding particle overlap. The box side was fixed to $L=1015$ in order to obtain a volume fraction of $\phi=0.0001$. To the best of our knowledge, these are the most diluted simulations of BDLCA performed so far (see Table I). In view of that, the system can safely be considered as representative of the ideal dilute regime. All particles are labelled with a property that we named charge. This property was allowed to have two possible values, +1 and −1, that correspond to the two different species of particles in a BDLCA process. The relative concentration, x, is an input value for the simulations.

All the particles and clusters were randomly moved with a size-dependent diffusion coefficient, D, that is related to the cluster radius of gyration R_g through the Stokes law, i.e., $D \propto R_g^{-1}$. In order to achieve BDLCA, the following reaction rules were imposed: (i) collisions between unlike particles always lead to bond formation and (ii) no bonds are allowed to form between like particles. The simulations do not account for possible rotation of the clusters. More details about this type of simulation can be found elsewhere [9–11].

The effective initial dimer formation rate, k_s, can be obtained from the monomer time evolution at short aggregation times, following the method reported by Drake [12]. It consists in a linear fitting of the $g(t)$ function, defined as

$$g(t) \equiv \frac{2V}{N_0}\left(\sqrt{\frac{N_0}{n_1(t)}}-1\right)=k_s t. \tag{8}$$

At sufficiently short times, when the linear fit holds, k_s can be identified with the slope of the fitting straight line.

Although Eq. (8) was derived for homoaggregation processes, $g(t)$ is always expected to behave linearly at short aggregation times when the aggregation processes start from monomeric initial conditions. In these cases, it should at least be possible to fit a straight line to the onset of $g(t)$. This procedure has been shown to be a suitable method for obtaining quite accurate k_s values from simulations and experiments, even when the aggregation kernel differed quite strongly from the constant kernel [11,13].

In a previous work [14], the described simulation method was used to determine the dimer formation rate constant under one-component diffusion-limited cluster-cluster aggregation (DLCA) conditions. The obtained value was $k_{11}^{\mathrm{Br}}=(10.778\pm0.017)10^{-18}\ \mathrm{m^3\,s^{-1}}$. This value is in excellent agreement with the theoretical prediction given by Eq. (7). The fitting error was estimated assuming a 95% confidence interval for the $g(t)$ function. For the given initial concentration, the characteristic aggregation time calculated by means of Eq. (5) was $t_{\mathrm{agr}}^{\mathrm{Br}}=(209.6\pm0.3)$ s.

IV. RESULTS AND DISCUSSION

A. Short time kinetics

BDLCA simulations were performed for a representative set of relative concentrations. The effective dimer formation rate constant, k_s, was calculated according to the method described in Sec. III. The fitting was restricted to a time interval of only 20 s in order to use only the most linear part of $g(t)$. This interval is about one order of magnitude smaller than the Brownian aggregation time. Due to that short time interval, the procedure was so accurate that the relative deviation was always smaller than 1%. Figure 1 shows the obtained k_s values as a function of the initial relative concentration. As predicted by the HHF theory, the effective dimer formation rate constant reach a maximum at $x=0.5$ where $k_s \approx \frac{1}{2}k_{11}^{\mathrm{Br}}$.

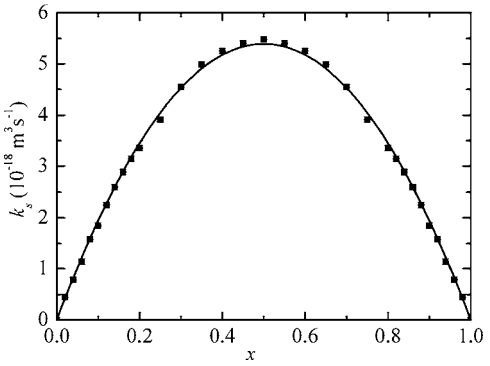

FIG. 1. Effective dimer formation rate, k_s, versus relative concentration, x, obtained from simulations (full squares) and the corresponding parabolic fit according to the HHF prediction (solid line).

It should be noted that simulation runs with a relative concentration x of particles of one type are, in turn, simulations with $1-x$ of particles of the other type. Accordingly, only the simulations with $x \leqslant 0.5$ were actually performed. Equation (6) was used to fit the obtained k_s data. As can be appreciated in Fig. 1, the corresponding parabolic fitting is excellent. Therefore, the HHF approximation is shown to be accurate for the early stages of BDLCA processes. The best fit was achieved for $k_{11}^{01}=(10.78\pm0.04)10^{-18}\ \mathrm{m^3\,s^{-1}}$. As expected, this value is exactly the Brownian aggregation rate constant k_{11}^{Br} obtained in previous DLCA simulations.

B. Long time behavior

In the very early stages of BDLCA processes, only reactions between monomers take place. This allowed an effective initial dimer formation rate constant, k_s, to be determined. As time goes on, however, reactions between clusters of any size occur and so, the complete set of reaction rate constants must be accounted for. This implies that it becomes a very challenging problem to obtain the complete aggregation kernel from experimental or simulated CSDs [15]. This is, of course, far beyond the scope of this work. Nevertheless, valuable information about the aggregation processes can be obtained directly from the cluster-size distributions without having to go through a detailed kinetic analysis.

Figure 2 shows the time evolution of the CSD for BDLCA processes starting from three significantly different initial relative concentrations $x=0.50$, $x=0.15$, and $x=0.05$. These values were chosen so that one lies clearly above, one close and one clearly below the critical relative concentration x_c. The plots show only the concentrations of the smaller clusters. One should, however, bear in mind that larger clusters are also present in the system. Their concentrations are

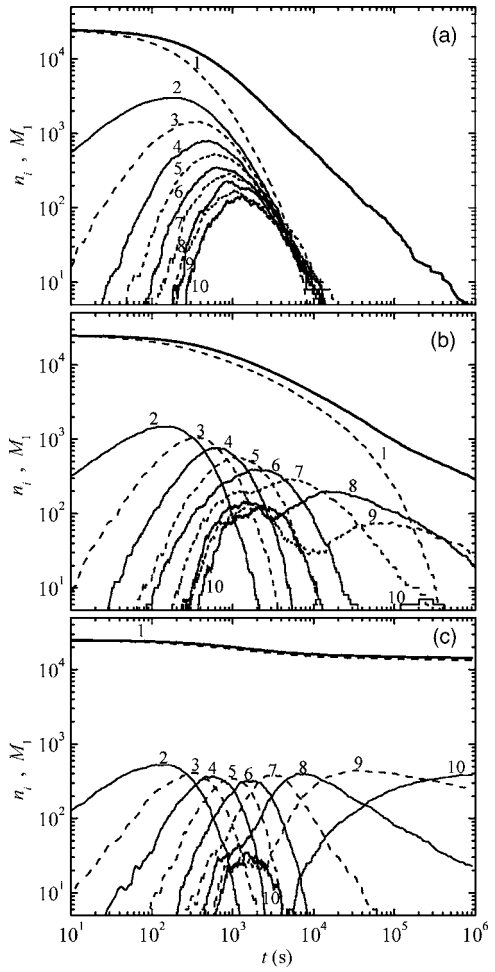

FIG. 2. Cluster size distribution up to 10-mers $n_i(t)$ (thin dashed lines for odd i and thin solid lines for even i), and the overall number of aggregates $M_1(t)$ (thick solid line), at the initial relative concentrations (a) $x=0.50$, (b) $x=0.15$, and (c) $x=0.05$. The numbers indicate the number of constituent particles of the clusters.

not plotted for the sake of clearness. Instead, the total number of clusters, $M_1(t)=\Sigma_{i=0}^{\infty} n_i(t)$, is included. As can be observed, the overall behavior of the CSD depends strongly on x. There are, however, some common features to all BDLCA simulations performed in this work, including those plotted in Fig. 2. (i) All of them start from monomeric initial conditions, $M_1(0)=n_1(0)=N_0$. (ii) The total number of aggregates decreases monotonically. In other words, the average cluster size always grows. (iii) While the number of monomers decreases monotonically, the number of larger aggregates reaches at least one maximum. (iv) The time at which these maxima are reached increases with the cluster size. The first three points are common to all systems that aggregate irreversibly starting from monomeric conditions.

In spite of these common features, there are substantial differences between the simulated BDLCA processes. One of the most outstanding points in this sense can be observed during the final stages of the aggregation processes. For relative concentrations around 0.5, the system reacts until all the particles are contained in a single large cluster. At very low x, this unique large cluster is never formed and a large number of aggregates and monomers remain in the system. Consequently, there must be a critical relative concentration x_c that divides both regions. As can be appreciated from Fig. 2, this critical point lies around $x=0.15$. At this relative concentration, a unique large cluster could be formed, but only at extremely large aggregation times.

We start the analysis of the obtained results discussing the CSDs that fall clearly in the single cluster forming region, well above x_c. At first sight, the time evolution of these CSDs seems to be very similar to the one obtained for fast aggregating one-component systems (DLCA). There are, however, significant differences that deserve to be discussed in more detail. Evidently, BDLCA is always slower than DLCA (see Sec. IV A) since only a fraction of all cluster-cluster encounters leads to bond formation. This effect is most pronounced for the smallest clusters, especially for monomers. The latter finding may be understood as follows: At $x=0.50$, e.g., one-half of all monomer-monomer encounters occur between like particles and so, cannot give rise to dimer formation. Larger clusters, however, may collide several times during an encounter [16]. Since they contain a similar number of particles of each type, it becomes quite likely that one of these consecutive contacts takes place between unlike particles. Consequently, two larger clusters will almost certainly aggregate once they encounter each other. This means that they behave almost like the sticky clusters in DLCA processes. Hence, BDLCA processes with a similar number of particles of each type are expected to cross over to DLCA after a certain time.

As mentioned before, one of the most important differences between BDLCA at $x\approx 0.5$ and DLCA kinetics lies in the clear excess of monomers. This monomer discrimination was recently observed in electrostatic heteroaggregation processes of dilute mixtures of oppositely charged colloidal particles when the experimental conditions came close to our simulation settings [17]. In these systems, the electrostatic interactions depend strongly on the electrolyte concentration of the aqueous phase. A BDLCA like regime was achieved at approximately 10 mM KBr, when the electrolyte concentration is low enough to prevent homoaggregation between like particles but high enough to avoid the long-range attraction between particles of opposite sign. As can be seen in Ref. [17] Fig. 2(b), the corresponding experimental CSD and our simulated data shown in Fig. 2(a) behave in a very similar way. This indicates that monomer discrimination has its origin solely in the reaction rules that are strictly fulfilled for monomers but can be overcome by the larger clusters due to multiple particle-particle contacts.

After having analyzed the single cluster forming region, we focus our attention on the results obtained for relative concentrations well below x_c. Figure 2(c) shows the CSD for $x=0.05$. A very unusual aggregation behavior is observed. For example, a large number of monomers remains in the system even at times as long as 10^6 s. These monomers are particles of the majority type that keep diffusing since they cannot find a free binding spot on a minority particle. Consequently, all the minority particles must be contained inside a shell of majority particles such that any further reaction becomes practically impossible. Since these clusters cannot react any more, we refer to them as stable aggregates. As can be appreciated in Fig. 2(c), the clusters composed by 9 and

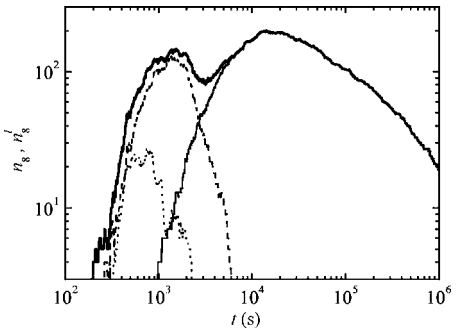

FIG. 3. Time evolution of the composition detailed cluster size distribution for octamers, $n_8^l(t)$, at $x=0.15$, $l=1$ (thin solid line), $l=2$ (dashed line), and $l=3$ (dotted line). The total number of octamers, $n_8(t)$, is also plotted (thick solid line).

10 particles have an extremely long lifetime and so, may be identified as such stable aggregates. These hardly reacting aggregates seem to be analogous to the stable oligomers reported by Djordjević [2] for on-lattice BDLCA simulations. We postpone the discussion about the behavior of these stable aggregates to Sec. IV C.

As stated before, the transition between the single cluster forming region and the stable cluster forming region is expected to lie close to $x=0.15$. The CSD for this relative concentration is shown in Fig. 2(b). Here, the total number of clusters decreases much slower than for $x\approx 0.5$. Moreover, an inflexion point is observed around $t=10^5$ s. This means that the aggregation process slows down even further after this point. Nevertheless, it is not clear what the final stage will be. The system might react until a single large cluster is formed. However, if that happened, an extremely long time would be required. Hence, the considered aggregation process shows characteristics of both, the single and the stable cluster forming region. The monomer concentration, e.g., decreases very slowly before the inflection point. After that, however, the monomers disappear completely.

One of the most interesting features of the aggregation processes in the transition region is observed for the 8-mers, 9-mers, and 10-mers. The numbers of these oligomers go through two clearly distinguishable maxima just like the humps of a camel. This reveals that there should be two aggregation mechanisms that take place at different time scales. It should be mentioned that such a clear double peaking behavior was not reported for on-lattice simulations. In fact, these two maxima correspond to two different oligomer compositions. As can be appreciated in the Fig. 3 for 8-mers, the short time maximum corresponds to clusters with two and three minority particles. The second maximum, however, is only due to octamers containing one minority particle. A similar behavior is found for 9-mers and 10-mers. The double peak formation is strongly related to the formation and growth of the stable aggregates and will be discussed later.

In order to identify the critical relative concentration x_c, it is convenient to analyze the long time behavior of the number of monomers $n_1(t)$ and the total number of aggregates $M_1(t)$. Both quantities are plotted in Fig. 4 for different values of x. Some free monomers are observed to remain in the

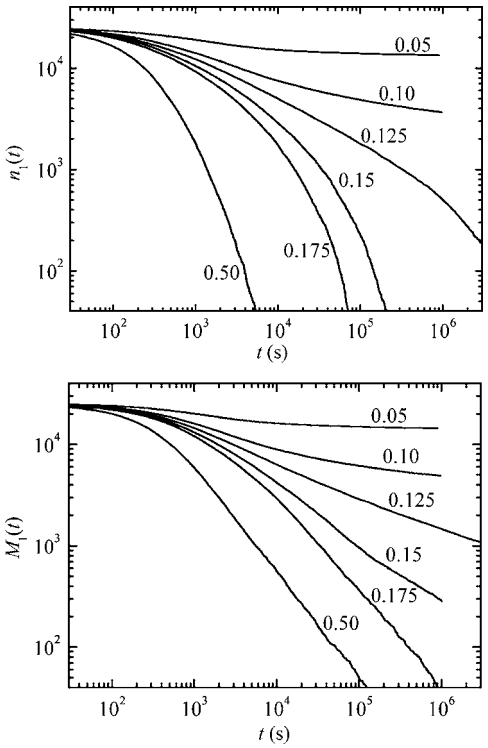

FIG. 4. Time evolution of the number of monomers (top) and the total number of aggregates (bottom) for different initial relative concentrations. The x values are indicated in the figures.

system for $x\leqslant 0.10$. Obviously, a unique aggregate will never be achieved in this case and so, the critical relative concentration x_c must be larger than 0.10. This lower limit is quite reasonable since it lies clearly above the theoretical limit of $1/13\approx 0.077$. The latter value is easily obtained if one takes into account that a minority particle can be covered by not more than 12 majority particles. Consequently, not all majority monomers can react if there are more than 12 majority particles per one minority particle.

Figure 4 also shows that the monomers tend to disappear completely for all relative concentrations above $x\geqslant 0.125$. Nevertheless, this value should not be taken as an upper limit for the relative concentration x_c since all the monomers could be arranged in stable aggregates that, however, will never form a unique cluster. This makes clear that the only way to determine the critical relative concentration x_c consists in analyzing the time evolution of the total number of aggregates.

According to Fig. 4, the total number of aggregates tends towards a value above unity for $x\leqslant 0.125$ while a clear tendency towards unity is observed for $x\geqslant 0.175$. As was mentioned before, the results for $x=0.15$ fall in a region where it is unclear what the final stage will be. Consequently, we only can ensure that the critical relative concentration x_c lies in the interval $]0.125, 0.175[$. It should be mentioned that Al-Sunaidi *et al.* obtained for the critical relative concentration an interval of $[0.190, 0.195]$ by means of on-lattice BDLCA simulations [1]. Their interval, however, lies clearly above the interval determined in this work by means of off-lattice simulations. This implies that the minority particles are on average covered by more majority particles when the particle position is not constrained to a cubic lattice.

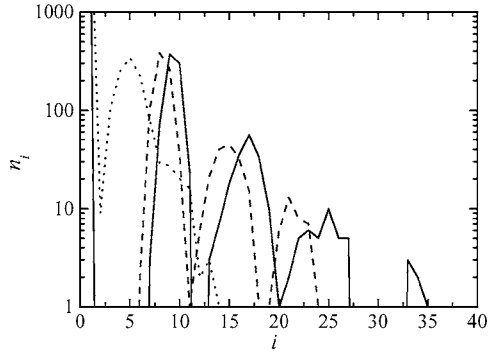

FIG. 5. CSD profile for simulated BDLCA with $x=0.05$ at different times, 10^3 s (dotted line), 10^4 s (dashed line), and 10^5 s (solid line). Please note that the number of monomers falls outside the plotted range.

Special attention should be payed to the lower limit of the critical relative concentration ($x=0.125$) where all the monomers will have reacted and form part of a relatively large number of stable aggregates. In other words, all the free majority particles will be bound in aggregates if minority particles are added to the system in a ratio of at least 15:100. Moreover, the production of those stable aggregates is most efficient in this case. Both findings might be useful for future industrial applications or serve as starting point for further research [18].

In the following section, we discuss the structure and growth of the stable aggregates that form at relative concentrations below x_c.

C. Stable aggregates

The stable clusters that remain in the system for relative concentrations below x_c are relatively small aggregates that are comprised by a few minority particles covered with a larger number of majority particles. In what follows, we will use the results for $x=0.05$ as a representative example of the whole stable cluster forming region. Figure 5 shows the cluster-size distribution profile at different times. As can be seen, the profile develops from its initial state towards a stable distribution characterized by several clearly distinguishable peaks. Each peak corresponds to aggregates with a fixed number of minority particles. We define the order of a cluster as its number of minority particles, i.e., all clusters having the same l in the $n_i^l(t)$ belong to the lth order. According to the figure, the first order aggregates peak around size 9. The second and third order peaks are centered around sizes of 17 and 25, respectively. The small number of aggregates of fourth order does not allow to determine the peak position reliably. Nevertheless, they seem to peak at size 33. A schematic view of typical aggregates from first to fourth order is shown in Fig. 6.

In on-lattice BDLCA simulations, there are well-defined binding spots on the particle surface that are given by the structure of the employed lattice. Unreactive or stable aggregates definitely remain in the system as soon as the binding sites on all minority particles are completely saturated by majority particles. At this final stage of BDLCA, the stable

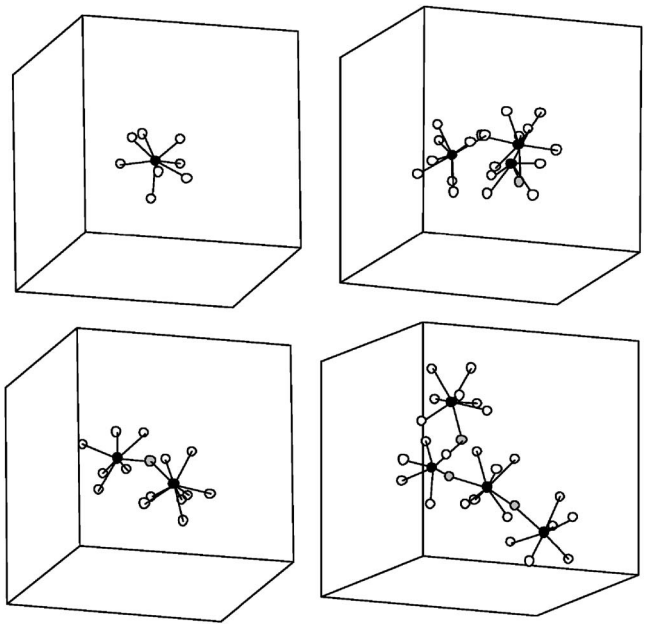

FIG. 6. Typical stable aggregates obtained by means of off-lattice BDLCA simulations with $x<x_c$. Black circles represent minority particles, gray circles represent majority particles that link two minority particles, and white circles represent other majority particles.

aggregates have a well-defined size and structure that depend on the type of the employed lattice. For a cubic lattice, e.g, stable aggregates of first order are always of size 7. Second order aggregates may have two different sizes depending on the type of bond that they contain. If the two minority particles are joined through a single majority particle, then, the resulting cluster size is 13. If they contain a double bond, i.e., the two minority particles bind simultaneously through two majority particles, the final cluster size is 12 [2].

When no lattice is imposed, however, there are no well-defined binding sites on the particle surface. Consequently, the structure and size of the stable aggregates is not predetermined. This implies that the stable aggregates that finally remain in the system have a wider size distribution. According to Fig. 5, the peaks for aggregates of first, second, and third order comprise the intervals [7, 12], [13, 20], and [20, 27], respectively. The lower limit for the size of the first order aggregates can be understood if one takes into account that it is possible to saturate a minority particle with just six majority particles if they are located on the vertices of an octahedron centered in it. The upper limit is determined by the densest possible packing of spheres that restricts the maximum coverage of a minority particle to 12 majority particles. Nevertheless, both limiting configurations are extremely ordered and so, very unlikely to observe in random process such as off-lattice BDLCA. In fact, we obtained only one stable aggregate of size 7 and none of size 13 in our simulations at $x=0.05$.

Figure 5 also shows that the peak structure of the CSD is well established at about $t=10^4$ s. As time goes on, the peak positions shift slightly towards higher sizes. The peak height, however, remains approximately constant. In order to quan-

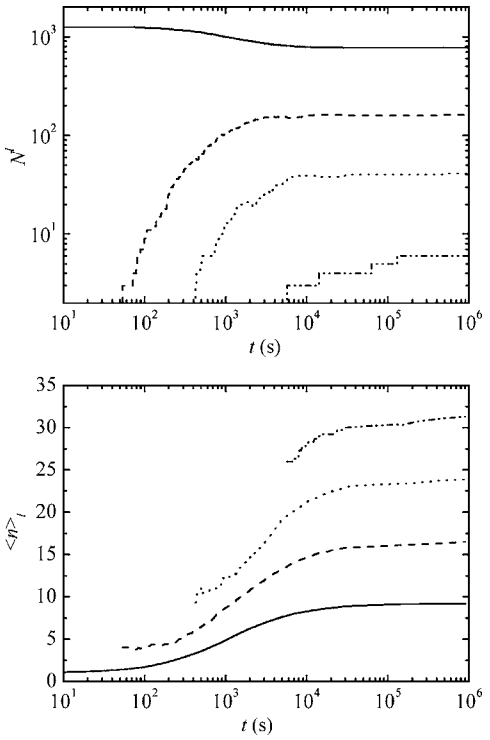

FIG. 7. Time evolution of the total number of aggregates of a given order (top) and their average size (bottom) obtained for $x=0.05$, for different l values, $l=1$ (solid line), $l=2$ (dashed line), $l=3$ (dotted line), and $l=4$ (dashed-dotted-dotted line).

tify this effect, we calculated the total number, $N^l=\Sigma_{i=1}^{\infty} n_i^l$, and the average size, $\langle n \rangle_l$, of all the aggregates of a lth order. The latter quantity is given by

$$\langle n \rangle_l = \frac{\sum_{i=1}^{\infty} i n_i^l(t)}{N^l(t)}. \tag{9}$$

The obtained results are plotted in Fig. 7. At long times, the number of clusters of each order remain constant although their sizes slightly increase. The mean size of the aggregates of each order correspond to the peak positions of Fig. 5. Furthermore, the different cluster orders seem always to be approximately equally spaced. This separation, however, increases in time. In the next section, we propose an aggregation model that tries to explain these findings.

D. Aggregation model for the stable cluster forming region $x<x_c'$

For a better understanding of the formation and growth of the stable aggregates at low x, it is convenient to study the time evolution of the total number of aggregates in the system and their average size. We exclude the monomers from these quantities in order to emphasize the behavior of the relatively few aggregates that form. Hence, the total number of clusters excluding monomers is given by

$$M_1(t) - n_1(t) = \sum_{i=2}^{\infty} n_i(t), \tag{10}$$

and the corresponding average aggregate size by

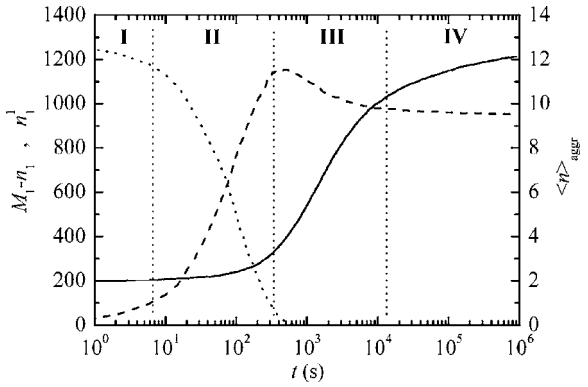

FIG. 8. Time evolution of the number of free minority particles n_1^1 (dotted line, left scale), the total number of clusters composed by more than one particle (dashed line, left scale) and their average size (solid line, right scale) for BDLCA with $x=0.05$. The vertical dotted lines indicate the different aggregation stages.

$$\langle n \rangle_{\text{aggr}} = \frac{N_0 - n_1(t)}{M_1(t) - n_1(t)}. \tag{11}$$

These two quantities and the number of free minority particles are plotted in Fig. 8 for simulated BDLCA processes at $x=0.05$. The curves allow us to distinguish several regions, labelled by roman numerals.

During the early stages of aggregation [stage (I)] the only possible reaction is dimer formation between minority and majority monomers. At very short times, $t \lesssim 5$ s, the number of minority monomers does not differ very much from its original value. This is the stage where the HHF approximation holds. Later [stage (II)], the total number of clusters increases quite fast while the average cluster size remains close to 2. This process continues until the free minority monomers disappear at approximately $t=3\times10^2$ s. At this time, the total number of aggregates reaches almost the number of minority particles. Consequently, all the minority particles have now reacted and are contained in small clusters. Only a very small number of larger aggregates may have formed so far. Since the majority of the formed aggregates contain only one minority particle they are first order seeds.

In the following region [stage (III)], the average cluster size starts to increase quite rapidly, while the total number of aggregates decreases slightly. This means that the formed aggregates or first order seeds grow mainly due to the addition of further majority particles. A few first order seeds, however, react among themselves forming aggregates that contain more than one minority particle. These higher order seeds will have a size of approximately a multiple of the average cluster size at that moment. This explains why aggregates of size 8 start to appear in the system when the predominant size of the first order seeds lies around 4 [see Figs. 2(c) and 7]. Evidently, the octamers formed at that stage will be mostly second order seeds.

The next aggregation stage (IV) starts at approximately $t=10^4$ s. At that time, the total number of clusters reaches a plateau while the average cluster size remains still somewhat increasing. This implies that the seeds do not react anymore among themselves but their size still increases due to the

addition of free majority monomers. Consequently, some majority monomers still find some open space or holes on the surface of the seeds where they can attach to minority particles. At this stage, the above-mentioned second order octamers will have grown up to fully developed second order aggregates with a size close to 17. At the same time, however, further octamers appear due to monomer addition to first order heptamers. This means that there are two octamers forming mechanisms that occur at very different time scales, (a) relatively fast second order seed formation and (b) quite slow first order seed completion. The combination of both mechanisms explains the camel-hump-like maxima mentioned in Sec. IV B (see Fig. 3). The first mechanism is of course the more pronounced the more minority particles are present in the system. The second mechanism occurs mainly when the number of first order seeds is much smaller than the number of majority particles. Close to the critical relative concentration x_c, the effect of both mechanisms is of the same order and this is why the camel-hump-like peaks in the CSD are observed best at $x=0.15$.

Finally, aggregation stops once all the holes on the surface of the seeds have disappeared. Our simulations, however, cannot unquestionably state this final point, but they give clear evidence. In summary, the proposed aggregation scheme for BDLCA processes for relative concentrations below x_c comprises the following five stages:

(I) HHF stage, fast reactions between unlike monomers form dimers.

(II) Seed formation stage, dimers keep being formed. They also grow by adding further majority particles and so become first order seeds. This stage ends when all free minority monomers have disappeared.

(III) Seed aggregation stage, some first order seeds react among themselves forming higher order seeds. These seeds keep growing by adding majority monomers.

(IV) Seed completion stage, the seeds are so highly covered that they cannot react any longer among themselves. Nevertheless, they still can grow by adding majority monomers.

(V) Stable aggregate stage, all clusters are completely coated by majority particles. Aggregation comes to an end.

This aggregation scheme is representative for all the simulated BDLCA processes for relative concentrations clearly below x_c. However, the moments at which these stages start and end, depend on the initial relative concentrations.

V. CONCLUSIONS

Binary diffusion-limited cluster-cluster aggregation processes were studied by means of off-lattice simulations. The fundamental role played by the relative concentration, x, was investigated for both, short and long aggregation times.

At short aggregation times, the predominant reaction is dimer formation due to bond formation between two unlike particles. In this region, the effective dimer formation rate constant, $k_s(x)$, follows the parabolic behavior predicted by the HHF approximation.

At long aggregation times, the aggregation behavior is highly dependent on x. For $x>x_c\approx 0.15$, aggregation continues until a single cluster is formed. In this region, the time evolution of the CSD is somewhat similar to the well-known DLCA processes. The main difference was found to be an excess of monomers that is observed even for $x=1/2$. This monomer excess seems to be identical to the monomer discrimination recently found in electrostatic heteroaggregation arising in oppositely charged colloids at low electrolyte concentrations [17]. In other words, our BDLCA simulations show that monomer discrimination may occur even in absence of any particle-particle interaction.

At x values close to x_c we found an atypical time evolution for oligomers composed from 8 to 10 particles: their number reached two maxima at different time scales. It is shown that these two maxima correspond to two different compositions: several minority particles per cluster at short times and just one minority particle per cluster at long times. This behavior was not reported for on-lattice BDLCA simulations.

At relative concentrations below x_c, stable aggregates remain diffusing in the system and a single cluster is never formed. In on-lattice simulations, the size and structure of these stable aggregates is restricted to a few fixed values that are determined by the structure of the imposed lattice. In off-lattice simulations, however, the stable aggregates group in wider bell-shaped distributions that correspond to clusters with a given number of minority particles. Furthermore, the minority particles are on average covered by more majority particles. Consequently, the critical relative concentration x_c reported in this work was found to be far lower than in on-lattice simulations.

We developed a five stage model for a suitable description of the formation and growth of stable aggregates in the low x region. Our model also explains the "two hump effect" for the oligomers. Finally, since real colloidal dispersions are not constricted to a lattice, we expect that experimental binary diffusion-limited heteroaggregation processes will be better explained by the results reported in this work. Such a comparison, however, will only make sense if the used experimental systems fulfill the BDLCA premises, i.e., short range interactions and strict selection rules. This can at least approximately be achieved in mixtures of oppositely charged colloids of similar size. According to the Derjagvin-Landau-Verwey-Overbeek (DLVO) theory, the range of the interactions in such electrostatically stabilized colloids depends on the electrolyte concentration of the solvent. At high electrolyte concentration, the interactions are very short ranged and attractive due to the London–van der Waals dispersion forces. At intermediate electrolyte concentrations, they are still short ranged but repulsive between like colloids and attractive between oppositely charged colloids. At very low electrolyte concentrations, the interactions are always long ranged. Our model should be applicable if both colloids are in the second region. There, the interactions are sufficiently short ranged so that the system is mainly diffusion controlled. The interactions are, however, still strong enough to ensure the selection rules to be strictly obeyed. Consequently, the system is expected to follow the BDLCA kinetics described in this paper. It is, of course, preferable to use oppositely charged colloids with similar surface potentials. Nevertheless, the surface charge ratio is not expected to play

an important role due to the short ranged interactions. Evidently, an extrapolation of the results to experiments should always be made with caution since remaining interactions may, e.g., alter the final structure of the stable aggregates and change the value of the critical relative concentration. In any case, our simulations give a clear idea what one expects in the limit of pure contact forces, i.e., extremely short range interactions.

ACKNOWLEDGMENTS

This work was supported by the Spanish "Ministerio de Educación y Ciencia" [Plan Nacional de Investigación Científica, Desarrollo e Innovación Tecnológica (I+D+i), project MAT 2003-08356-C04-01] and by the "European Regional Development Fund" (ERDF).

[1] A. AlSunaidi, M. Lach-hab, A. E. González, and E. Blaisten-Barojas, Phys. Rev. E **61**, 550 (2000).
[2] P. Meakin and Z. B. Djordjević, J. Phys. A **19**, 2137 (1986).
[3] S. Stoll and E. Pefferkorn, J. Colloid Interface Sci. **160**, 149 (1993).
[4] A. M. Puertas, A. Fernández-Barbero, and F. J. de las Nieves, Colloids Surf., A **195**, 189 (2001).
[5] M. von Smoluchowski, Phys. Z. **17**, 557 (1916).
[6] M. von Smoluchowski, Z. Phys. Chem., Stoechiom. Verwandtschaftsl. **92**, 129 (1917).
[7] F. Leyvraz, Phys. Rep. **383**, 95 (2003).
[8] R. Hogg, T. W. Healy, and D. W. Fuerstenau, Trans. Faraday Soc. **62**, 1638 (1966).
[9] P. Meakin, Z. Chen, and J. M. Deutch, J. Chem. Phys. **82**, 3786 (1985).
[10] A. E. González, Phys. Rev. Lett. **71**, 2248 (1993).
[11] A. Moncho-Jordá, G. Odriozola, M. Tirado-Miranda, A. Schmitt, and R. Hidalgo-Álvarez, Phys. Rev. E **68**, 011404 (2003).
[12] R. L. Drake, in *Topics in Current Aerosol Research*, edited by G. M. Hidy and J. R. Brock (Pergamon, New York, 1972).
[13] H. Holthoff, A. Schmitt, A. Fernández-Barbero, M. Borkovec, M. Á. Cabrerizo-Vílchez, P. Schurtenberger, and R. Hidalgo-Álvarez, J. Colloid Interface Sci. **192**, 463 (1997).
[14] A. Schmitt, G. Odriozola, A. Moncho-Jordá, J. Callejas-Fernández, R. Martínez-García, and R. Hidalgo-Álvarez, Phys. Rev. E **62**, 8335 (2000).
[15] D. Ramkrishna, *Population Balances: Theory and Applications to Particulate Systems in Engineering* (Academic, New York, 2000).
[16] G. Odriozola, A. Moncho-Jordá, A. Schmitt, J. Callejas-Fernández, R. Martínez-García, and R. Hidalgo-Álvarez, Europhys. Lett. **53**, 797 (2001).
[17] J. M. López-López, A. Schmitt, J. Callejas-Fernández, and R. Hidalgo-Álvarez, Phys. Rev. E **69**, 011404 (2004).
[18] V. N. Manoharan, M. T. Elsesser, and D. J. Pine, Science **301**, 483 (2003).